Chapter 4
3D Hand Geometry Recognition

Michal Dvořák and Martin Drahanský

1 Introduction

How can a person be reliably identified or verified and how secure is this method? The area of biometrics offers a solution to this issue by claiming that to determine one's identity, only some of his/her physical traits are needed. Many security systems of today identify people using various biometrics, most often fingerprint, facial markers, or retina scan. These systems, however, are not applicable in every situation either due to environmental, price, or other reasons, and another method may be required. Hand geometry represents an alternative approach to human identification and verification that avoids issues that make more conventional approaches inconvenient, such as placement in areas where the face needs to be covered or where fingerprints can become obscured (non-clean environment).

The fundamental idea of hand-based geometry identification is built around the assumption that everyone possesses a hand and its shape is unique. In other words, if a reference shape of user's hand is on record, this person's identity can be established by comparing his immediate hand shape with the one on record. It was this assumption that gave birth to the first systems designed to do just so.

The first problem that needs to be solved is to identify the characteristics that can be both efficiently collected without compromising the requirement for uniqueness. 2D hand geometry then represents a viable abstraction method where the parameters are such as silhouette or length, width, and thickness of fingers [1].

In order to expand into a 3D system, a measurement of depth has to be introduced; this then in turn allows parameters such as curvatures of individual fingers and wrist as well as plastic deformations on the back or palm of the hand to be measured.

M. Dvořák (✉) · M. Drahanský
Brno University of Technology, Centre of Excellence IT4Innovations, Brno, Czech Republic
e-mail: idvorakmi@fit.vutbr.cz; drahan@fit.vutbr.cz

M. S. Obaidat et al. (eds.), *Biometric-Based Physical and Cybersecurity Systems*,
https://doi.org/10.1007/978-3-319-98734-7_4

2 2D Hand Geometry Acquisition

To better understand the issues presented by hand biometrics, let's first take a brief look on principle of 2D acquisition.

The method itself is tantalizingly simple, since all that is needed is a silhouette of a hand. For this task, all that is required is a CCD or CMOS camera with sufficient resolution, and whereas for fingerprint identification, this resolution may be high and thus require a more expensive sensor, e.g., 500 DPI; the hand geometry systems will operate with much lower-resolution cameras in commercial systems usually 100–200 DPI but viable with even less than 100 DPI [2].

During 2D acquisition a static image of a back of a hand is usually captured, which is followed by the extraction of required features. Depending on system, additional images may be acquired from different angles in order to gather additional features. This usually takes form of capturing the image from the top and side in order to gain all previously mentioned features [1]. As can be seen on Fig. 4.1, image from this direction allows for efficient gathering of majority of required features.

The system may be further modified to improve the acquisition process and simplify the feature extraction stage, such as including reflective background to enhance edges or add cameras to have more sources of features and pins which ensure that the hand is in a predictable position; the principle however remains the same. Figure 4.2 shows the possible set of features to be extracted. All of currently available solutions are based on this principle.

2.1 Existing Commercial Solutions

As far as authors are concerned, there are to this day only two commercial systems being currently developed, both under the Schlage. These are devices of HandPunch® and HandKey® series, respectively.

At the time of writing this chapter, the newest model of the series was HandKey II [3], HandPunch GT-400 [4], and HandPunch 4000 [5]. HandKey II, as can be seen

Fig. 4.1 Gathered image of a hand for 2D hand geometry extraction of features

on Fig. 4.2, is foremost an access device, designed to primarily serve as a security access mechanism which is the reason why it has features such as duress code. The base user memory of the device is 512 user fields which is expandable. Per available information, the hand geometry features are after extraction compressed to 9 byte large template.

The HandPunch series is per description to primarily serve as a time and attendance terminal. HandPunch 4000, like the HandKey II, employs 9 byte large template size; the default user memory is 530, with offered expandability to 3498. The HandPunch GT series differs in design but appears to be similar in function. The template size is different, as it is represented by 20 bytes instead of 9 bytes. The device also has a larger default user field size of 1000 and no offer of expansion. On Fig. 4.3 the appearance of HandPunch device can be seen.

Fig. 4.2 Image of HandKey II biometrics hand geometry reader [3]

Fig. 4.3 Image of HandPunch GT-400 biometrics hand geometry reader [4]

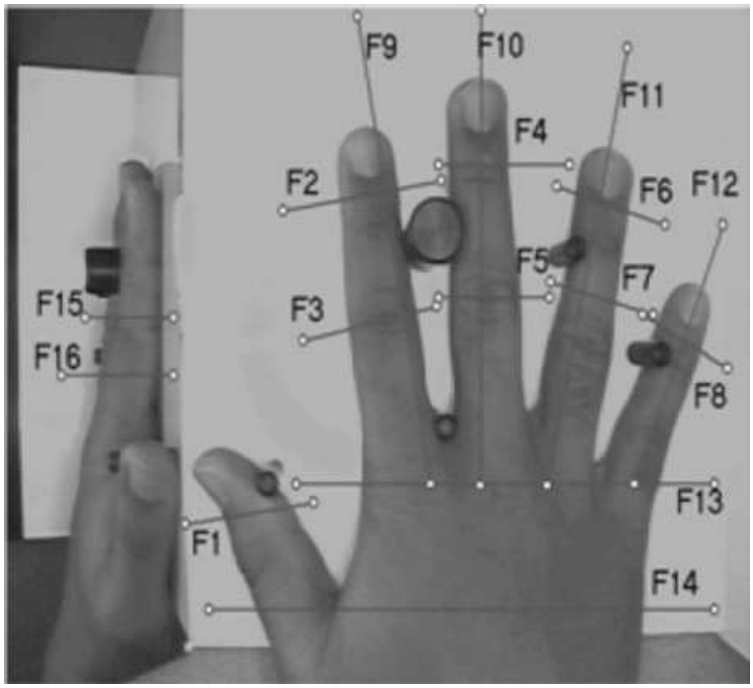

Fig. 4.4 Viable hand 2D hand geometry features [2]

2.2 *Identification Methods*

To identify a user based on their hand geometry, methodology needs to be devised to extract unique set of features, by which comparison of one set can be determined to belong to the same person. Since the likelihood of the source images being completely identical is minute, due to small placement and orientation differences, as well as small changes in hand shape over time, the methods need to accommodate a tolerance in the measurements. In general, methods based on direct measurements and hand shape alignment are used today.

2.2.1 Methods Based on Direct Measurement

In this case, a vector of dimensions is constructed based on measurements gained directly from the acquired image of a person's hand. As can be seen, for example, on Figs. 4.4 and 4.14 features can be directly inferred from downward-facing camera and additional 2 from side-facing camera. All the commercially available systems appear to utilize solely the upward-facing camera. The features themselves can either be extracted from a binary image after the segmentation of the hand from the background or they can be calculated from the defined pixel ranges. It is worth mentioning that while the number of features that can be extracted from image is nearly limitless, very little additional useful information is gained with increased number of features (Fig. 4.5).

During the matching phase, the two feature vectors, one of the newly measured hand and the other of saved template, are compared against each other based on a chosen metrics, such as sum of absolute difference (1), weighted sum of absolute

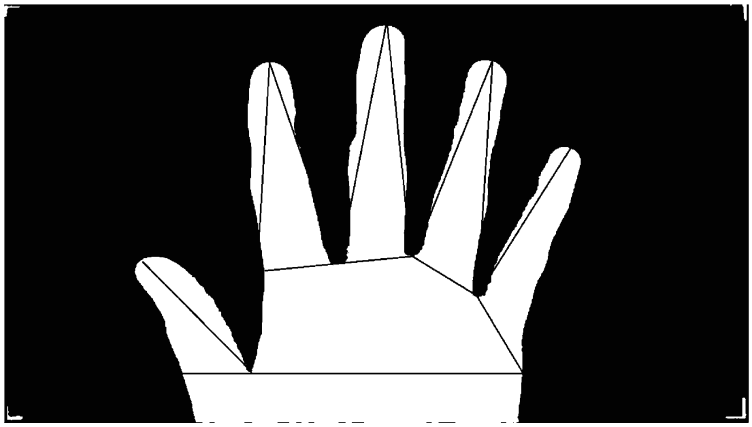

Fig. 4.5 Other possible set of extractable features

difference (2), Euclidean distance (3), or weighted Euclidean distance (4) [1]. The measured features are defined as $x_i = [x_1, x_2, \ldots, x_z]$, template features as $y_i = [y_1, y_2, \ldots, y_z]$, and σ_i as a weight of the given feature.

$$\sum_{i=1}^{z} |x_i - y_i| \tag{4.1}$$

$$\sum_{i=1}^{z} \frac{|x_i - y_i|}{\sigma_i} \tag{4.2}$$

$$\sqrt{\sum_{i=1}^{z} (x_i - y_i)^2} \tag{4.3}$$

$$\sqrt{\sum_{i=1}^{z} \frac{(x_i - y_i)^2}{\sigma_i^2}} \tag{4.4}$$

Both advantage and disadvantage of this method are the requirement for pins. For the feature extraction, same set of pixels is used every time, since the range of movement of the hand is restricted by these pins. The pins are accomplished by guiding the hand into a predefined position. The advantage is that this method is fast and/or requires very low computational power as there is no need to algorithmically determine the position of each feature. The disadvantages are the pins themselves; the necessity of them prevents the method to become touchless and disqualifies the usage of dynamic acquisition, as it requires proper position before the image is acquired. And while the commercial devices have an antibacterial layer, it still can be a potential health risk.

The shortcomings of this method can be addressed by methods based on silhouette matching.

2.2.2 Methods Based on Silhouette Alignment

In this method, fixed position is not required, even though it can be applied even to a pin-guided system. Instead of measuring fixed distances, , a measure of difference

between a new outline/silhouette of a hand and the outline stored as a template, is calculated.

The general steps of this method are as follows:

- Preprocessing based on the chosen system.
- Outline extraction, since the object should be easily separable from background, only a preferred method of thresholding is required to acquire a binary image and usage of morphologic operations to gain an outline of the measured hand.
- Finger extraction, the outlines of individual fingers need to be extracted. To identify them, tips and valleys of the fingers are detected. This step is especially necessary in pinless systems.
- Align the corresponding finger pairs with template. To do this, any algorithms that measure distance of two metric subspaces can be used, for example, modified Hausdorff distance [6] where the orientation and position of one outline are gradually changed to achieve closest alignment with the reference.
- Calculate the distance of the pair. MAE (*mean alignment error*) is then calculated, an average distance difference between corresponding points of the outlines.
- If MAE is less than the decided threshold, it is declared that the measured hand is of the same person as the one saved in template.

On Fig. 4.6 the fingers of measured hand aligned on top of the template saved in database can be seen. MAE would now be calculated, and based on thresholding it would be decided whether the analyzed hand matches the template. (In this case it clearly does not.)

While both these methods serve the purpose they are designed for, they do exhibit several limitations.

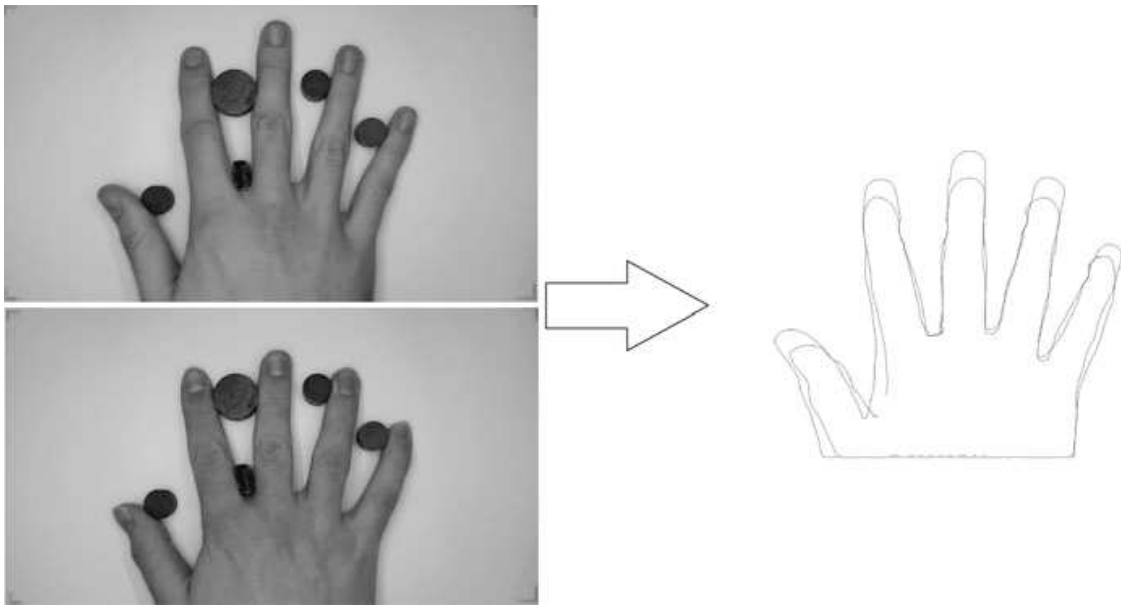

Fig. 4.6 – Hand image used as a source and second hand image (left), outline overlap after finger positioning (right)

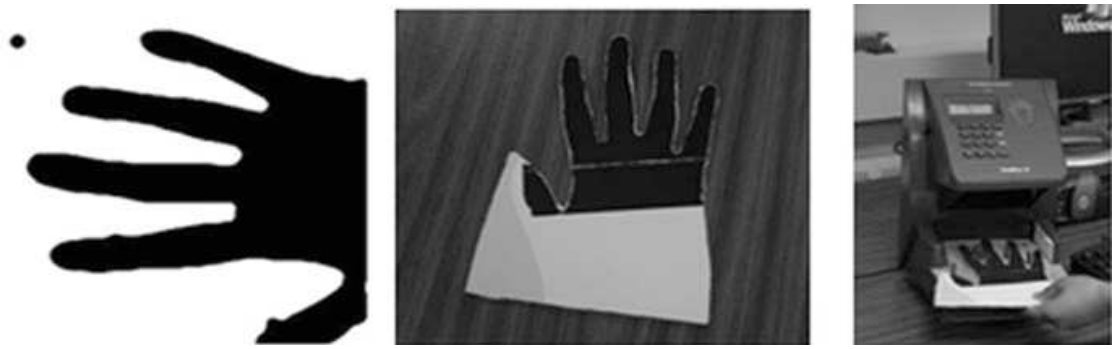

Fig. 4.7 Paper silhouette spoof used to bypass commercial device [8]

2.3 Limitations of Currently Employed 2D Hand Geometry-Based Biometrics

The simplicity of acquisition and low demands on the resolution of the sensor present are, however, several shortcomings; while some are still being addressed, others are insurmountable due to the limitations of 2D acquisition .

Despite the improvement of existing commercial hand recognition tools such as HandKey II [3], due to the fact that only relatively small amount of information is available to begin with, either the database size or success rate of identification has to be sacrificed, as proved by the continued research into uniqueness of one's hand and its measurements as viable identification parameter of large population [7]. The transition from 2D to 3D hand recognition adds features and feature vectors, thus increasing an entropy and offering a solution to the issue.

Spoofing presents another challenge as was demonstrated in [8] where a simple paper silhouette was used as a spoof that could be used to introduce a successful impostor. To detect a spoof, the system has to be able to acquire data that is difficult to replicate when developing a spoof, either by including detection of large amount information or by detecting a property of human hand that is inherently unavailable in an artificial spoof, such as detecting whether currently analyzed object is in fact part of the living human body (Fig. 4.7).

The approaches to verifying liveliness of hand are multiple; among the most common are the approaches based on detecting body heat for confirmation, which however increases complexity and costs of the system, especially of system that is to be touchless. The resistivity/conductivity of the human skin can be used as well; it too however imposes the requirement for the system to be touch based. From the optical approaches, which would meet the criteria for making the system touchless, is the most common one, the utilization of vein detection. This can be achieved either by a surface detection utilizing a near-infrared light (NIR) or subsequent detection, i.e., Fig. 4.8.

Alternatively, system can capture a dispersed light passing through the hand as in Fig. 4.9. With this approach, usually only fingers are used as the whole hand presents too much tissue for the NIR and the absorption of NIR by hemoglobin is no longer

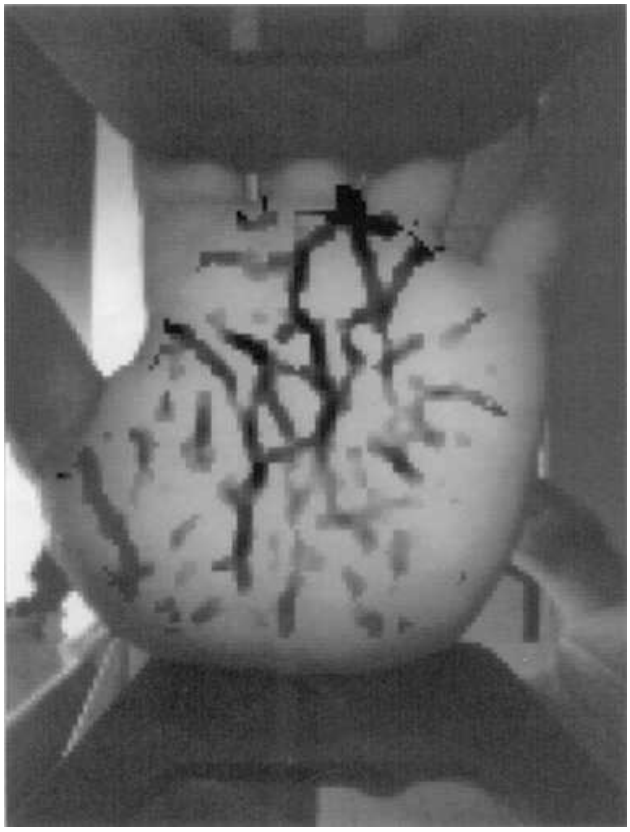

Fig. 4.8 Surface vein detection using NIR

Fig. 4.9 Vein detection using NIR light source behind object

easily detectable without special light source. Either of these approaches is easily implementable into the hand biometric system, as the NIR can be used as a light source in CCD- or CMOS-based systems. The vein detection can then be used either as only a liveliness verification or preferably as an additional source of unique and identifiable features.

The multidimensional approach can assist by increasing the amount of information needed for construction of spoof. Necessary dimensions gathering from uncooperative target become a nontrivial task, as a majority of 3D scanning approaches requires scanned object in a specific position or the accuracy will decrease. As far as authors are concerned to date, no one has presented a method of acquiring a 3D scan of a hand from an uncooperative user with accuracy necessary to create a viable spoof. As will be explored further in subsequent parts of this chapter, the experiments have been performed in this area and support the assumption of increased entropy.

The last limitation that needs to be mentioned here is the difficulty in creating a pinless and contactless solution. As far as the authors are concerned, there are no existing pinless and by extension contactless commercial devices available now. While the issue of pinless hand recognition has been approached even in pure 2D hand recognition systems, it has been demonstrated that utilization of depth sensing devices is a viable method of approaching this problem [9] as well as the need for the physical contact with the sensing device.

3 3D Acquisition

The principle of 3D acquisition in biometrics has been successfully tested. The price and high computational demands limited these tests to academic research in the past. However, as the price of viable 3D acquisition devices keeps decreasing and the computational capabilities of even mobile hardware increasing, the 3D acquisition has become a viable alternative to 2D hand geometry systems.

On Fig. 4.10 a 3D image captured using low-cost Creative VF0800 camera [10] can be seen. On the image, it can be seen that, along with required 3D features, majority of 2D features can be inferred as well, which allow extraction of the 3D and

Fig. 4.10 3D image of hand using low-cost 3D camera

2D features with no additional hardware. As the depth map also includes information necessary to determine absolute dimensions of scanned object, it can also be used as a basis for a contactless system.

While any 3D mapping method may be used, in 3D hand geometry, it can be observed that majority of academic publications use a system based on principle of active triangulation, be it the industrial 3D laser digitizers [11, 12] or systems based on light pattern projection [13].

3.1 Using 3D Scanner

Utilization of professional laser scanner in biometrics can be seen in [11] – in this case a Minolta Vivid 910 has been used for creation of large database (3540 items) of right hand scans, where the device can work with accuracy in three axes up to X, 0.22 mm; Y, 0.16 mm; and Z, 0.10 mm to the Z reference plane [14].

The method presented in [11] localizes the position of four fingers on intensity map and based on this information extracts corresponding data from range map. The cross sections of each finger are extracted at chosen distances along the finger's length. This paper then proceeds to calculate features based on curvature and vector of normal of the finger segment. Figure 4.11 shows a depth data of cross section, calculating curvature and normal features.

In the paper, the 2D and 3D data is experimentally matched, and EER (equal error rate) and AUC (area under ROC curve) are calculated (Table 4.1).

As expected, the combined 2D and 3D geometry data provides the best performance.

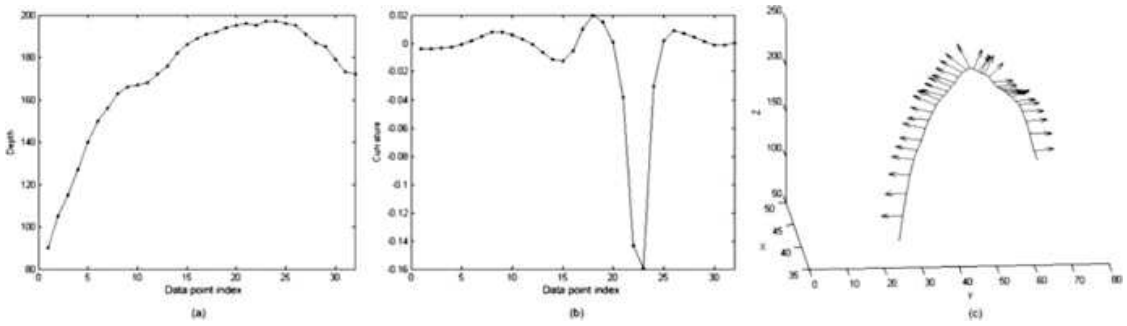

Fig. 4.11 (**a**) Cross-sectional finger segment and (**b**) its computed curvature features; (**c**) normal features computed for a finger segment [12]

Table 4.1 EER and AUC of 2D, 3D, and a combined matcher [12]

Matcher	EER [%]	AUC
3D hand geometry	3.5	0.9655
2D hand geometry	6.3	0.9722
(2D + 3D) hand geometry	2.3	0.9888

3.2 Using Structured Light

The use of structured light is based on the projection of visible or infrared pattern of defined properties onto a surface of an object, in our case a human hand. On the surface of a plastic object, the pattern appears deformed; by recording the direction and magnitude of this deformation, and comparing it to expected position, the depth of the pixel can be calculated. This approach has been used in several publications, where various sources of the pattern have been tested.

3.2.1 IR Pattern Projection

This approach became viable thanks to the spread of affordable 3D cameras such Intel RealSense or Microsoft Kinect. The cameras in this case provide both an RGB image and a depth map, with corresponding coordinates.

In [12] it was demonstrated that by using Intel RealSense camera, 2D and 3D features may be collected. After the preprocessing, during which markers such as fingertips, finger valleys, and wrist lines are identified, a vector including 41-dimensional vector of 2D features and 137-dimensional vector of 3D features can be extracted. Features are:

- Finger length (2D)
- Finger valley distance (2D)
- Finger width (2D)
- Wrist to valley distance (2D)
- Finger axis surface distance (3D)
- Finger width (3D)

Figures 4.12 and 4.13 show the respective features on the depth images and intensity images.

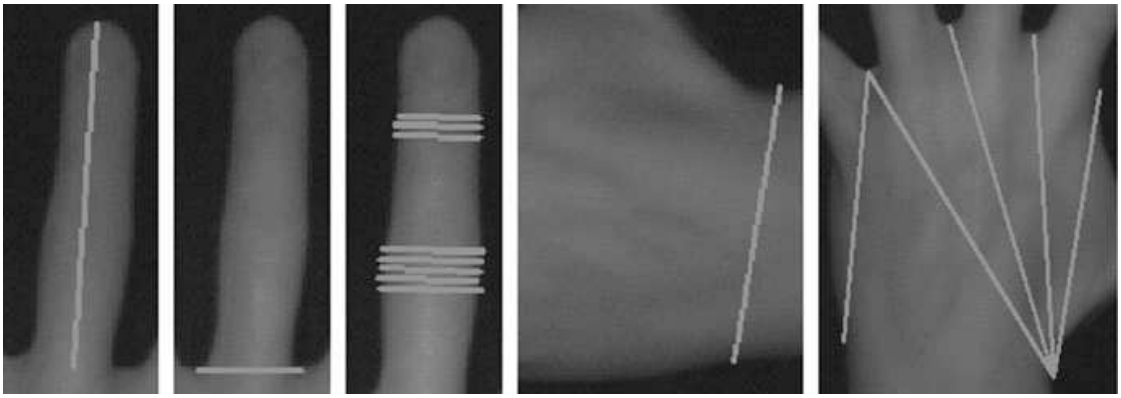

Fig. 4.12 Extracted 2D features [13]

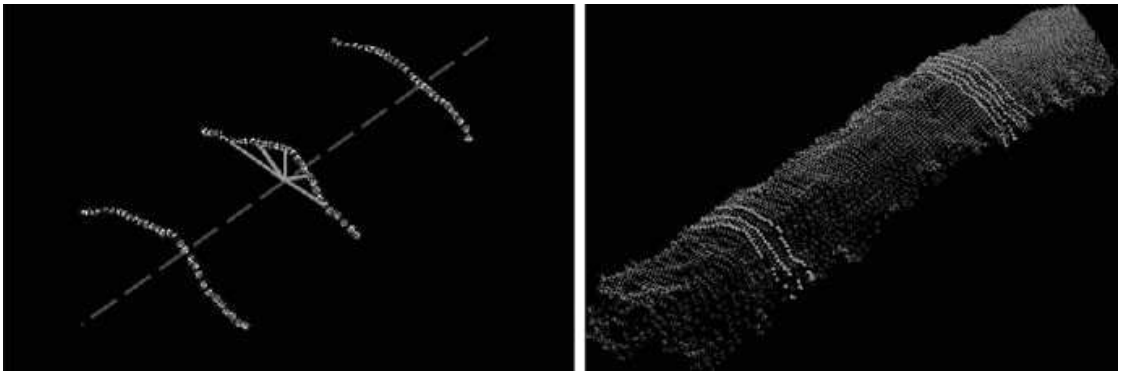

Fig. 4.13 Extracted 3D features [13]

Table 4.2 Overall performance of Bronstein and Drahansky system using LMNN metric learning approach [12]

		FRR [%]	
Features	ERR [%]	@FAR = 0.5%	@FAR = 1%
2D	2.76	6.50	1.63
3D	2.92	10.70	6.42
2D + 3D	1.61	4.81	2.23

Table 4.3 Qualitative comparison of hand biometric-based matchers [12]

Method	Features	Templates	Database	FAR [%]	FRR [%]	EER [%]
Jain and Duta	2D	1–14	53	2.00	3.50	N/A
Jain et al.	2D	1 (avg)	50	2.00	15.00	N/A
Woodard and Flynn	2D + 3D	1 (avg)	177	5.50	5.50	5.50
Malassiotis et al.	2D + 3D	4	73	3.60	3.60	3.60
Kumar et al.	2D + 3D	5	100	5.30	8.20	N/A
Kanhangad et al.	2D + 3D	5	177	2.60	2.60	2.60
Bronstein and Drahansky	2D + 3D	1 (avg)	88	1.61	1.61	1.61

The feature vectors are in this case matched using the *Mahalanobis distance* [15], utilizing *large margin nearest neighbors* (LMNN) [16] the weights for individual features.

As the 2D and 3D feature vectors are calculated separately, a comparison of individual vector performance as well as the performance of their combination can be examined (Table 4.2).

From these data, it can be inferred that while 3D features alone with low-cost hardware, in combination with 2D features, the resultant method proves superior. The improvement is especially apparent in case of images where one of the source vectors suffers high level of noise. Where second stream serves to improve to overall recognition rate, this method proved to be comparable even with the state-of-the-art approaches (Table 4.3).

3.2.2 Lasers and Diffraction Grating

A shortcoming of generic commercial light pattern-based approach is its lack of detail and operation on short range, and even though the results were still satisfactory, the system can be improved upon by designing the light projection for the application. Both the wavelength and the actual pattern can then be chosen, based on a priory information about the measured object.

In [17] the array of 532 nm lasers is being used with simple two MS LifeCam HD 3000 camcorders used for acquisition. Optics on laser turns the dot projection into line projection, and diffraction grating then allows to turn the single line into an array of parallel lines. On Fig. 4.14, it can be observed how the resultant line pattern appears on hand and how it can be separated from the background.

As can be seen, on Fig. 4.15 the concept has been proven, and the model of 3D hand may be reconstructed despite the low cost of entire setup.

So far, this method has only been presented as a viable scanning method and no database has been produced. As is, the method performs a preprocessing necessary for 2D hand geometry identification and thus can be seen as a viable approach to

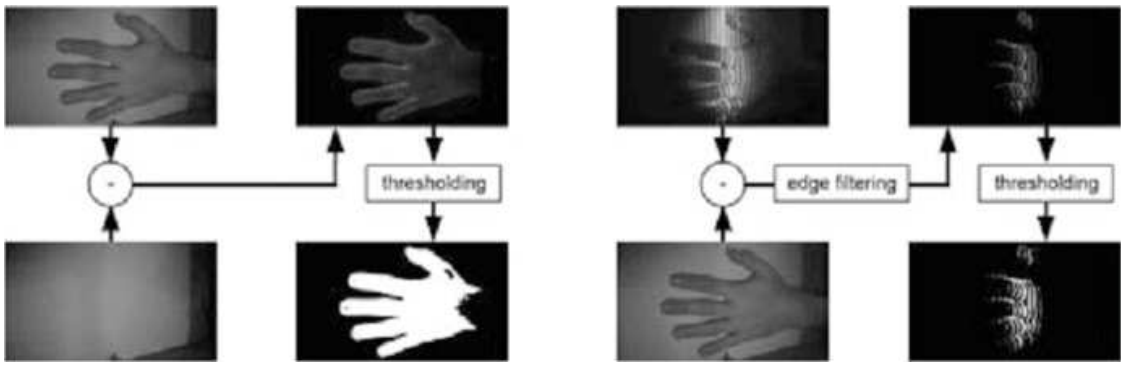

Fig. 4.14 The process of extracting the deformation markers, created by diffracting line projection [17]

Fig. 4.15 Resultant surface reconstruction from the line projection [17]

increasing the entropy of the hand biometrics. The accuracy of method has been demonstrated by scanning an object of known dimensions.

The cube with side of length 25.5 mm has been scanned, and the root mean squared and normalized root mean squared have been calculated (Table 4.4).

3.3 Time-of-Flight (TOF) Scanning

TOF cameras due to the principle of their operation are more suited for scanning large objects. However with emergence of low-cost systems such as SoftKinetic DS325 and Kinect v2 RGB-D camera, even this form of image capture has become available.

While the research in hand biometry using the TOF has been limited solely to gesture detection, there has been an investigation on potential biometric applications, especially with regard to face recognition [18]. The use of TOF cameras has been tested in order to capture a depth map of user's facial features from various technologies, as can be seen on Fig. 4.16.

Various approaches to filtering 3D meshes have been investigated, such as feature preserving mesh denoising, and show that despite the high noise level, the information can be extracted with accuracy high enough for rudimentary biometric identification (Fig. 4.17).

Table 4.4 Accuracy of the proposed method based on calibration [17]

Model	NRMSE	RMSE
Laser 0	0.2190	1.4558
Laser 1	0.1993	0.7977
Laser 2	0.1764	0.4317
Merged	0.1764	1.0474

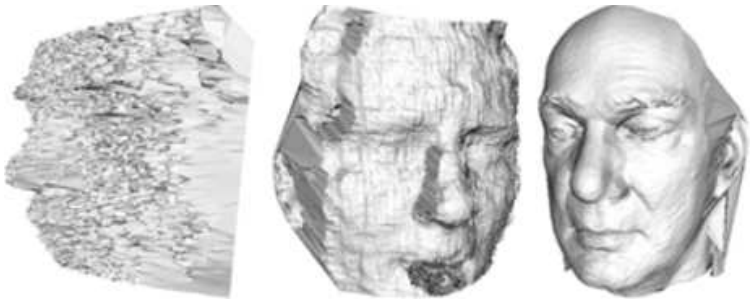

Fig. 4.16 Example 3D acquisition using TOF cameras SoftKinetic (left), Kinect (middle), and professional Minolta Vivid scanner (right) [18]

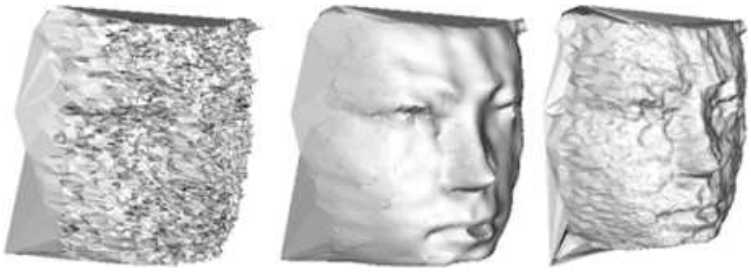

Fig. 4.17 High-noise DS325 image (left), after application of feature preserving mesh denoising (middle) and Gaussian smoothing (right) [18]

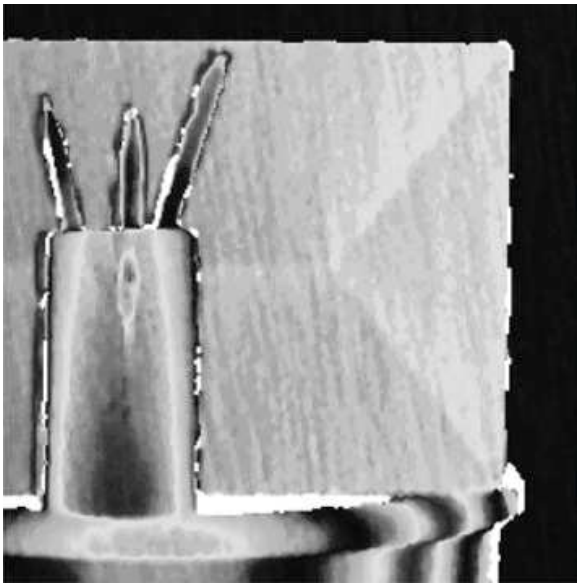

Fig. 4.18 Example of 3D image created using stereovision [20]

3.4 Stereovision Approach

Stereo vision utilizes multiple cameras fixed in known position. Due to a distance between them, an observed object will appear displaced on the two images acquired from two cameras. The magnitude of this displacement can be used to calculate a position of the object in three axes, and if resolution is high enough, the shape of an object can be determined, as the deformations too appear displaced on two images.

Currently there are multiple produces offering a 3D stereo image acquisition with declared resolution high enough for biometric usage, for example, ENSENSO N10-304-18 with resolution in Z axis up to 0.109 mm [19]. The most prevalent issue of stereovision technology appears when scanning homogenous object; however, as the hand due to papillary lines is not homogenous, this issue in our case does not apply. In theory any calibrated two camera setup can, given enough information, generate a 3D model using specialized software (Fig. 4.18).

To bypass homogeneity, random noise projection is sometimes used. By projecting the noise onto the object, the parallax calculation can be calculated for every visible projected pixel.

4 Utilization of Line Scanners in Biometric Acquisition

Direction in image acquisition that is now being explored by the authors is utilization of line scanners for 2D and 3D multimodal hand biometrics. The advantages present themselves in the form of acquisition of a dynamic object (hand). This would lead to increasing a throughput at a gate utilizing this system, while maintaining image quality necessary for multimodal feature extraction, namely, fingerprints and palm prints.

4.1 Camera System

The proposed goal of this system is to be able to perform an image acquisition such that 2D hand geometry can be extracted, with resolution and accuracy high enough to allow for subsequent fingerprint and palm print recovery with a hand moving up to 0.5 ms^{-1}. The system also must be expendable to allow for 3D hand geometry features to be extracted.

To meet these demands, a line scanner would need to be capable of output resolution of 500 DPI on the cross section of at least 200 mm, requiring the physical resolution of at least 4000 px. To meet the vertical resolution requirement, with the same output resolution requirement, the minimum required framerate is 10 kHz.

The Basler racer raL6144-16gm [21] has been chosen, as the 6144 ph resolution is sufficient and as 17 kHz frame rate would allow for hand moment of up to 850 mms^{-1}. Secondary reason for choosing this model is the sensor size of 43 m, allowing for utilization of full-frame optics.

The optics have been chosen based on the requirements for maximum distance of object from sensor and especially with depth of focus in mind, in order to accommodate the touchless requirement for the system. AF Nikkor 50 mm f/1.8D has been determined to meet these requirements.

4.2 Proof of Concept

Figure 4.19a) shows an image acquired via line scanner fixed on a moving platform moving at a speed of 0.5 m/s. Figure 4.19b) then focuses on a detail of a little finger, demonstrating that output resolution is high enough for a fingerprint extraction and therefore high enough for 2D hand geometry extraction. Due to high noise of the background, ideal segmentation is not trivial, and for demonstration on Fig. 4.20, a mask has been used to remove majority of generated noise.

To demonstrate the possibility of fingerprint extraction, we have used the commercial tool VeriFinger [22]. As can be seen on Fig. 4.21, as expected, the setup being realized as proof of concept only, the lighting proved to be non-ideal and produced glare resulted in a void appearing in the segmented picture of the fingerprint. At the same time however it can be noticed that there is a large number of positively identified fingerprint markers, serving as proof that the system as is is sufficient for the defined task.

Palm print feature extraction can be performed in a similar manner, as the lighting in the POC was not ideal for this sort of data processing and voids can be observed due to glares; overall, however, it can be confirmed that this setup is viable for palm print extraction as well, thus allowing a statement that the POC has met the requirement placed on it. Figure 4.22 presents an image ready for palm print feature extraction.

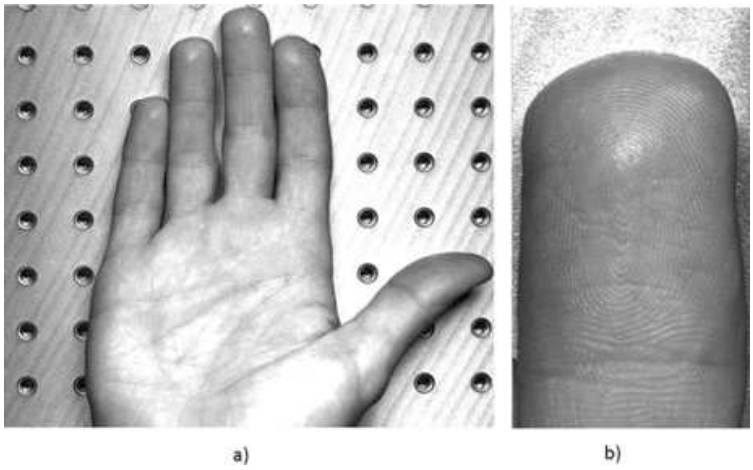

Fig. 4.19 (**a**) Palm print using line scanner mounted on moving platform; (**b**) detail of ring finger

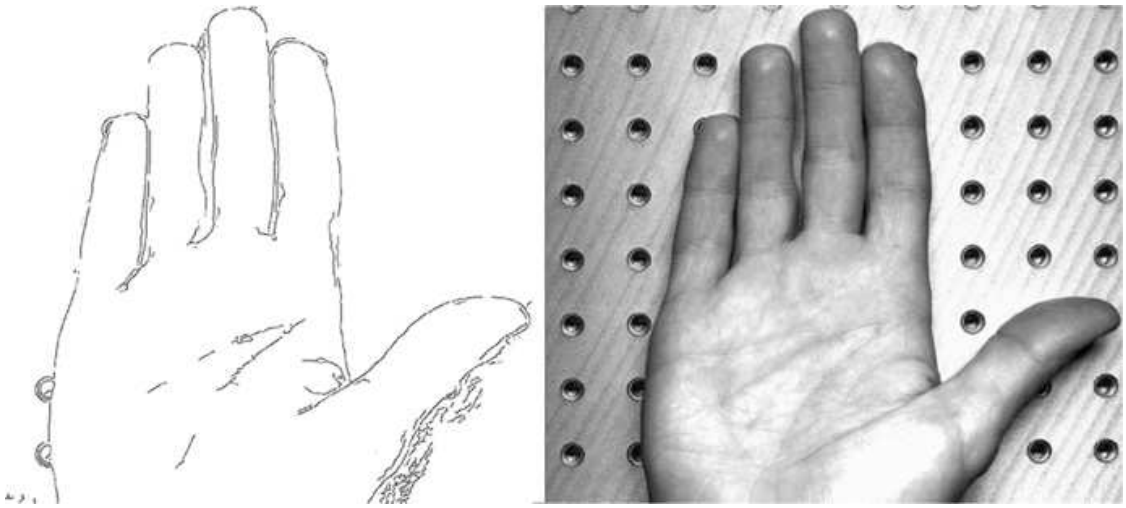

Fig. 4.20 Mack filtering and edge detection used to extract outline (left) from an image of hand acquired via line scanner (right)

Fig. 4.21 Fingerprint image using line scanner (right), extracted fingerprint using VeriFinger SDK (right)

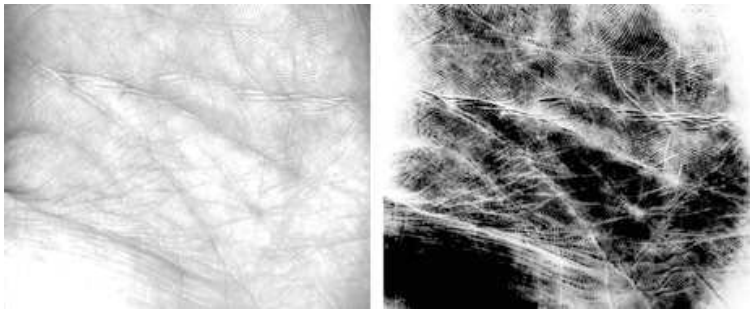

Fig. 4.22 The POC palm print extraction from the image, source image (left) and preprocessed palm print (right)

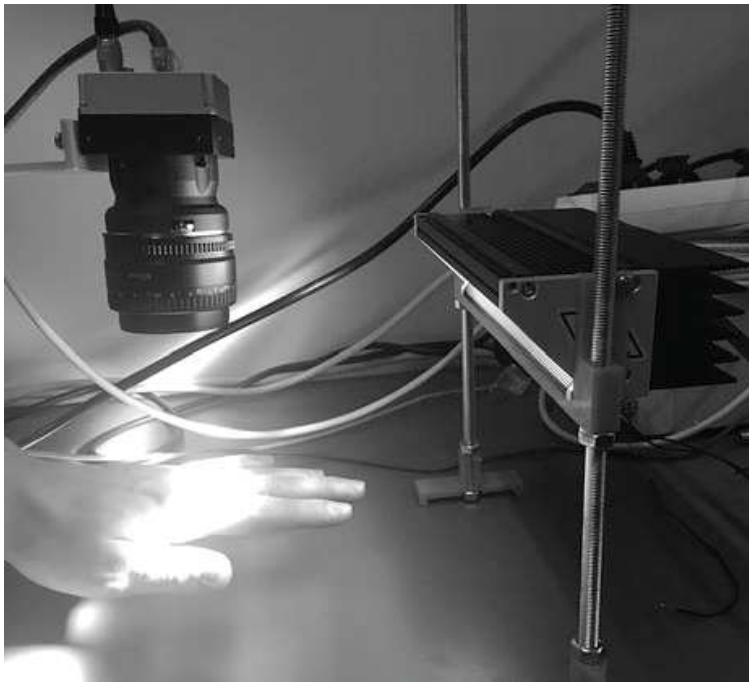

Fig. 4.23 Setup of system with free-hand movement

4.3 Reconstruction of Hand Image in Touchless System

Reconstruction of hand model using a data from a non-calibrated movement is currently being explored. Based on the proof of concept, a camera system has been constructed, which allows a free movement of the hand under the field of view of the line scanner, unlike POC where the hand was moving at constant speed while fixed to the moving platform. The setup is presented on Fig. 4.23.

Initial tests with this setup have been performed, and as can be seen on Fig. 4.24, the uneven movement speed and direction lead to deformations that make hand geometry extraction complicated; however, the overall details presented serve as proof of viability of this method for biometric feature extraction.

4.4 Utilization of 3D Line Scanner of 3D Feature Extraction

As has been briefly mentioned in the earlier part of the chapter, stereovision is one of the possible approaches in acquiring the 3D features of hand geometry. 3D PIXIA

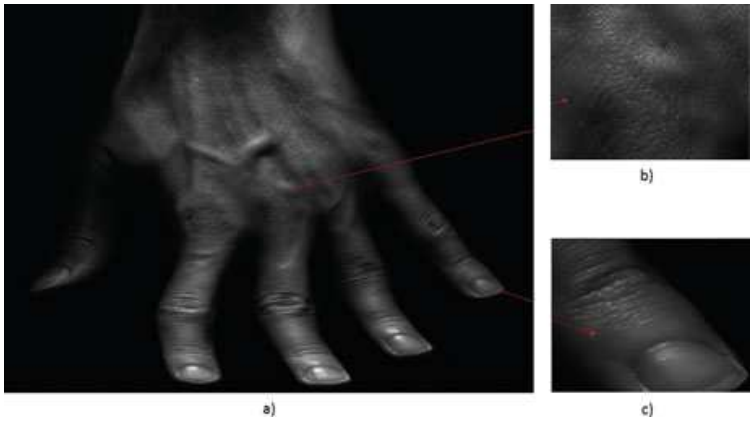

Fig. 4.24 (**a**) Handprint using a fixed line scanner scanning a moving hand; (**b**) detail of middle knuckle; (**c**) detail of little finger

Fig. 4.25 Preview of 3DPIXA setup for 3D line scan acquisition

[23] has been identified as a camera, whose specification parameters meet the requirements necessary for accurate 3D feature acquisition (Fig. 4.25).

As of now, only theoretical and preliminary preparations have been made.

5 Conclusion

In this chapter, an overview of current state of development in 2D and 3D hand-based biometrics has been presented. Existing methods of 2D acquisition and identification have been described as well as systems that are now available commercially. The shortcomings of 2D-based biometrics especially in relation to their susceptibility to spoofing have been explored, and possible approaches to solving these shortcomings with existing methods that allow for more secure system were established.

3D-based geometry has been introduced as a viable direction in development, and advantages of this method presented over 2D geometry have been outlined. Current development in this area has been presented, as well as other viable methods that warrant a future research.

Novel method of biometric image acquisition has been presented, utilizing line scanner. The design and test of proof-of-concept device have been shown. The capability of multimodal acquisition has been demonstrated by performing a test extraction of palm print, fingerprint, and outline of a hand captured by this system. Expansion of this system that would allow for extraction of 3D features has been discussed.

3D hand geometry biometrics builds upon the 2D hand geometry a good method for biometrics. 2D method has proven to be useful in applications where other methods of identification are inconvenient. It has been unable to become truly widespread, due to limited template size. With the advance of 3D approach, this wish could become rectified and allow this technology to spread.

Acknowledgment This work was supported by the Ministry of Education, Youth and Sports from the National Programme of Sustainability (NPU II) project IT4Innovations excellence in science, LQ1602, and "Secure and Reliable Computer Systems" IGA – FIT-S-17-4014.

References

1. M. Drahanský, F. Orság, et al., *Biometrie* (Computer Press, Brno, 2011). ISBN 978-80-254-8979-6
2. A.K. Jain, A. Ross, S. Pankanti, A prototype hand geometry-based verification system, Proc. AVBPA (1999), pp. 166–171,
3. HandKey II, *Allegion* [online]. Dublin, Ireland (2014) [cit. 2017-04-25]. Available at: http://us.allegion.com/Products/biometrics/handkey2/Pages/default.aspx
4. HandPunch GT-400, *Allegion* [online]. Dublin, Ireland (2014) [cit. 2017-04-25]. Available at: http://us.allegion.com/Products/time_attendance/g_series/gt400/Pages/default.aspx
5. HandPunch 4000, *Allegion* [online]. Dublin, Ireland (2014) [cit. 2017–04-25]. Available at: http://us.allegion.com/Products/time_attendance/f_series/hp_4000/Pages/default.aspx
6. M.-P. Dubuisson, A.K. Jain, A modified Hausdorff distance for object matching. Pattern Recognition, 1994. Vol. 1-Conference A: Computer Vision & Image Processing., in *Proceedings of the 12th IAPR International Conference on*, Vol. 1. IEEE, (1994)
7. M.A. Ferrer, J. Fabregas, M. Faundez, J.B. Alonso, C. Travieso, Hand geometry identification system performance, in *43rd Annual 2009 International Carnahan Conference on Security Technology*, Zurich, (2009), pp. 167–171
8. H. Chen, H. Valizadegan, C. Jackson, S. Soltysiak, A.K. Jain, Fake hands: spoofing hand geometry systems, in *Biometric Consortium 2005*, (Washington, DC, 2005)
9. S.-I. Joo, S.-H. Weon, H.-I. Choi, Real-time depth-based hand detection and tracking. Sci. World J. **2014**, 284827, 17 pages (2014). doi:https://doi.org/10.1155/2014/284827
10. Intel RealSense™ Camera [online] (2015), [cit. 2017–04-17]. Available at: https://software.intel.com/en-us/RealSense/SR300Camera
11. V. Kanhangad, A. Kumar, D. Zhang, Combining 2D and 3D hand geometry features for biometric verification, in *2009 I.E. Computer Society Conference on Computer Vision and Pattern Recognition Workshops*, (Miami, FL 2009), pp. 39–44
12. V. Kanhangad, A. Kumar, D. Zhang, A unified framework for contactless hand verification. IEEE Trans. Inf. Foren. Sec., 6 (3), 1014–1027 (2011)). https://doi.org/10.1109/TIFS.2011.2121062
13. J. Svoboda, M. Bronstein, M. Drahanský, Contactless biometric hand geometry recognition using a low-cost 3D camera, in *Proceedings 2015 International Conference on Biometrics*, (IEEE Biometric Council, Phuket, 2015), pp. 452–457 ISBN 978-1-4799-7824-3

14. Vivid 910: Non-contact 3D digitizer [online]. In (2002), s. 6 [cit. 2017-04-17]. Available at: http://www.upc.edu/sct/documents_equipament/d_288_id-715.pdf
15. P.C. Mahalanobis, On the generalised distance in statistics (PDF). Proc. Nat. Inst. Sci. India **2** (1), 49–55 (1936). Retrieved 29 Sept 2016
16. K.Q. Weinberger, J.C. Blitzer, L.K. Saul, Distance metric learning for large margin nearest neighbor classification. Adv. Neural Inf. Proces. Syst. **18**, 1473–1480 (2006)
17. J. Svoboda, O. Klubal, M. Drahanský, Biometric recognition of people by 3D hand geometry. in *The International Conference on Digital Technologies 2013*, Zilina, (2013), pp. 137–141
18. Š. Mráček, et al., 3D face recognition on low-cost depth sensors. Biometrics Special Interest Group (BIOSIG), in *2014 International Conference of the. IEEE* (2014)
19. Ensenso N10. *Imaging development systems* [online]. Obersulm, Germany [cit. 2017-04-25]. Available at: https://en.ids-imaging.com/ensenso-n10.html
20. Nové modely 3D kamer Ensenso. Analyza obrazu [online]. (2015) [cit. 2017-04-25]. Available at: http://www.analyza-obrazu.cz/aktuality/nove-modely-3d-kamer-ensenso/
21. RaL6144-16gm - Basler racer. Basler: The power of sight [online]. Germany [cit. 2017-04-25]. Available at: https://www.baslerweb.com/en/products/cameras/line-scan-cameras/racer/ral6144-16gm/
22. VeriFinger SDK. Neurotechnology [online]. [cit. 2017-04-25]. Available at: http://www.neurotechnology.com/verifinger.html
23. 3D Line Scan Camera 3DPIXA compact 30µm. Chromasens [online]. [cit. 2017-04-30]. Available at: https://www.chromasens.de/en/product/3d-line-scan-camera-3dpixa-compact-30um